Ion implantation and pulsed laser melting processing for the development of an intermediate band material

E. García-Hemme, R. García-Hernansanz, J. Olea, D. Pastor, A. del Prado et al.

Citation: AIP Conf. Proc. **1496**, 54 (2012); doi: 10.1063/1.4766488
View online: http://dx.doi.org/10.1063/1.4766488
View Table of Contents: http://proceedings.aip.org/dbt/dbt.jsp?KEY=APCPCS&Volume=1496&Issue=1
Published by the American Institute of Physics.

Ion Implantation and Pulsed Laser Melting Processing for the Development of an Intermediate Band Material

E. García-Hemme[1, 2], R. García-Hernansanz[1, 2], J. Olea[2, 3], D. Pastor[1, 2, 3], A. del Prado[1, 2] , I. Mártil[1, 2], G. Gónzalez-Díaz[1, 2].

[1]*Dept. de Física Aplicada III (Electricidad y Electrónica), Univ. Complutense de Madrid, 28040 Madrid, Spain*
[2]*CEI Campus Moncloa, UCM-UPM, 28040 Madrid, Spain*
[3]*Instituto de Energía Solar, E.T.S.I. de Telecomunicación, Univ. Politécnica de Madrid. 28040 Madrid, Spain*

Abstract. Ti supersaturated Si layers with two different thicknesses have been obtained on the top of a Si substrate by means of ion implantation and pulsed laser melting processes. Time-of-flight Secondary Ion Mass spectrometry (ToF-SIMS) measurements show Ti concentration above the intermediate band formation limit. This feature has been obtained in 20 nm for one of the set of samples and in 120 nm in the other one. Sheet resistance measurements at variable temperature show an unusual electrical decoupling between the Ti implanted layer and the n-Si substrate in the two sets of samples. This behavior has been successfully explained using the intermediate band theory. These results points out that we have achieved thicker layers of intermediate band material.

Keywords: Silicon, Titanium, Ion Implantation, Pulsed Laser Melting, Solar Cell, Intermediate Band.
PACS: 85.40.Ry – 73 – 73.81.05.Cy – 81.05.Zx – 81.10.Fq – 52.77.Dq

INTRODUCTION

Our current energy model based on the massive consumption of fossil fuels has proved once and again to be incompatible with a sustainable development of our society. The scientific community is devoting a tremendous effort in the development of new technological concepts to obtain a more efficient and environmentally friendly energy system based on renewable energy sources.

In the field of solar energy, a third generation of photovoltaic devices is about to come with higher conversion efficiencies and a better use of the solar spectrum. In this context, the intermediate band (IB) solar cell is one of the most promising ideas. In a traditional solar cell, only those photons with energy equal or higher than the band gap could be used to excite electrons from the valence band (VB) to the conduction band (CB). However, we do not take advantage of those photons with energy lower than the band gap. In an IB material, a new band of allowed states is formed within the semiconductor band gap. In this scenario, photons with energy lower than the band gap could be used to excite electrons from de VB to the IB and from the IB to the CB. This extra photocurrent would be added to that given by transition VB – CB leading to an increase in the photo-generated current and higher conversion efficiencies [1].

There exist some different approaches to obtain an IB material as the quantum dots and high mismatched alloys [2, 3]. In this work we are going to deal with the deep levels approach. This method consists in the introduction of a high amount of deep levels impurities in a host semiconductor. As the impurity concentration increases they would begin to interact due to the spatial proximity. The deep levels associated with these impurities would begin to overlap, and due to the Pauli Exclusion Principle, a splitting of the discrete deep level would occur. This phenomenon would lead to localization – delocalization transition and a band of allowed states would be formed within the band gap of the host semiconductor [4]. This concentration limit is known as the Mott limit and has been theoretically calculated (~$6x10^{19}$ cm^{-3}) [5].

In the particular case of this research we have selected Si as host semiconductor since it would be very interesting to extend the very mature Si solar cell technology to the fabrication of IB Si based solar cells. We have selected Ti due to theoretical studies based on quantum calculation that have predicted the IB formation in Si samples with Ti concentrations above the Mott limit [6].

However, to achieve this high impurity concentration we have to surpass the solid solubility limit of Ti in Si (10^{14} cm^{-3}) [7], which is several orders of magnitude lower than the Mott limit. We need to introduce a Ti concentration in the Si crystalline structure at least five orders of magnitude higher than the maximum Ti concentration allowed in thermodynamical equilibrium. Additionally, the final processed material has to present a high crystalline quality and a thick layer in order to be used in a high efficiency photovoltaic device implementation.

Ion Implantation Technology 2012
AIP Conf. Proc. 1496, 54-57 (2012); doi: 10.1063/1.4766488

Techniques in thermodynamical equilibrium would not be suitable to fabricate an IB material since the Si lattice will not allow this high Ti concentration. Ion implantation appears in this scenario as a powerful tool to introduce the desired concentration of the impurity ion and to select with accuracy the final depth within the host semiconductor.

However, crystal damage is inherent to any ion implantation process. Annealing in thermodynamical equilibrium is not a suitable option to recover the lattice crystallinity since Ti concentration is over the solid solubility limit in Si. This kind of processes would make Si to expulse a high concentration of the implanted Ti or would allow the formation of secondary phases likes Ti silicide. Conversely, out of the thermodynamically equilibrium processes as the Pulsed laser melting (PLM) would have the required properties. PLM process consists of a high energy density laser spot that focuses on the material in an extremely short time in the order of nanosecond. A superficial layer is then melted: in liquid phase the diffusion coefficient and solubility limit are orders of magnitude higher than in solid phase, allowing the impurities to spread in the layer homogeneously. By an explosive solidification, the layer recrystallizes using the seed of the non-implanted Si substrate region and therefore crystalline Si substrate. This process allows a high solute trapping of the Ti impurities and permits to overcome the solid solubility limit obtaining an excellent crystal quality [8].

EXPERIMENTAL

Samples 1x1 cm^2 in size of n-type Si (111) with a thickness of 300 µm (ρ≈200 Ωcm; µ≈1500 cm; n≈2x10^{13} cm^{-3} at RT) were implanted in a refurbished VARIAN CF3000 Ion Implanter. One set was single Ti implanted at 25 KeV with a 10^{15} cm^{-2} dose while the other set was double Ti implanted at 35 KeV and 150 KeV with doses of 10^{15} cm^{-2} and 4x10^{15} cm^{-2} respectively. All samples were implanted using a 7° tilt angle to reduce possible channeling effects. After implantation, all the samples were PLM processed with one 20 ns long pulse at an energy density of 0.8 J/cm^2 for the single implantation case and 1.8 J/cm^2 for the double implanted samples. The system was a KrF excimer laser (248 nm) at J.P. Sercel Associates Inc. (New Hampshire, USA). Finally, 100 nm Ti plus 200 nm Al were evaporated as four small triangular contacts by means of the e-beam method in the sample corners to electrically characterize the samples by the van der Pauw technique.

Electrical characterization was made at variable temperature (100 – 300 K) placing the samples inside a homemade liquid nitrogen cryostat. In order to avoid moisture condensation, the cryostat was attached to a vacuum pump. A Keithley SCS 4200 model with four source and measure units was used to perform the sheet resistance measurement with the van der Pauw configuration.

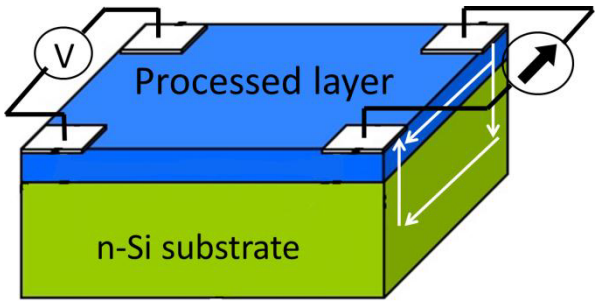

FIGURE 1. Schematic 3D view of the van der Pauw set-up.

In Fig. 1 we represent a schematic 3D view of the van der Pauw set up used for the sheet resistance measurements. We introduce the current using two contacts at the Ti implanted layer (TIL) corners and measure the voltage using the opposite two contacts. With this scheme we assume a parallel electrical conduction scheme. Namely the current will flow from one electrode to the adjacent electrode through the TIL and the Si substrate.

To analyze the Ti depth profile, time-of-flight secondary ion mass spectrometry (ToF-SIMS) measurements were carried out in a ToF-SIMS IV model manufactured by ION-TOF, with a 25 keV pulsed Bi^{3+} beam at 45° incidence. A 10 keV voltage was used to extract the secondary ions generated and their time of flight from the sample to the detector was measured with a reflection mass spectrometer.

RESULTS

In Fig. 2 we observe the ToF – SIMS Ti concentration depth profile of the two set of implanted samples before and after the PLM process. For the two set of samples it can be clearly seen that Ti concentration reaches values over the Mott limit. Specifically we obtain Ti concentration over the theoretical Mott limit after the PLM process in a thickness of approximately 20 nm for the simple implanted set of samples and 120 nm for the double implanted set of samples.

A strong push out effect of the impurities to the surface producing a superficial Ti concentration peak is clearly observed for the two set of samples after the PLM process. In the case of the simple implanted set of samples we observe two Ti concentration peaks, one very superficial at 10 nm with Ti concentration over the Mott limit and the other one at 50 nm and with Ti concentration below the Mott limit. Between

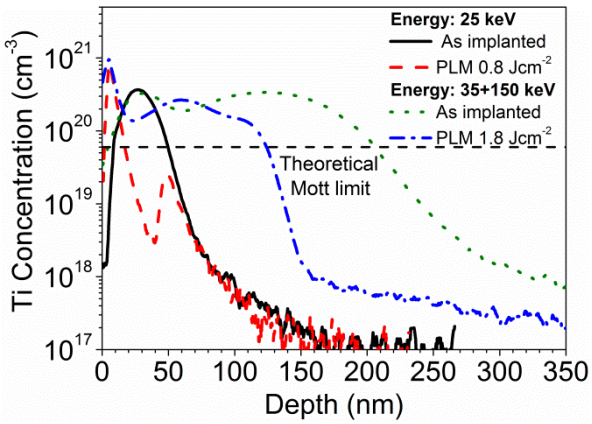

FIGURE 2. ToF-SIMS Ti concentration depth profile of two set of implanted samples before and after PLM. One set was PLM processed at 0.8 Jcm^{-2} and the other at 1.8 Jcm^{-2}.

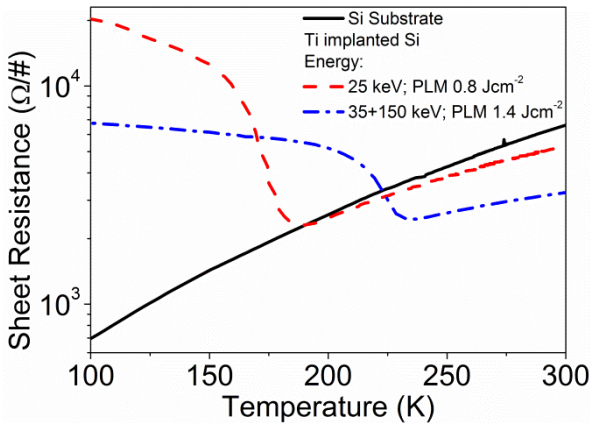

FIGURE 3. Sheet resistance as function of temperature measured for the two set of implanted and PLM samples.

these two peaks a separating valley appears at a depth of 40 nm. This valley indicates the beginning of the solidifying front, from where the superficial 40 nm has been melted while the layer beyond has been only heated but not melted. In the case of the double implanted sample the valleys do not appear and a box-shaped depth profile can be clearly observed [9, 10]. This shows that a region deeper than the implanted layer has been melted. Crystalline recovery has been studied in similar implanted samples by means of electron diffraction, transmission electron microscopy and glancing incidence X – ray diffraction showing that after the PLM process, a high crystalline structure is obtained [10, 11]. In a detailed Raman spectroscopy characterization no evidences of secondary phase formation (like Ti silicides) has been observed in samples with similar implanted doses [12].

In Fig. 3 we represent the sheet resistance measurements as a function of the measured temperature for the two implanted samples and for a Si reference sample. At low temperatures we observe the decrease in the sheet resistance for the Si reference sample. This is the expected behavior due to the reduction of the optical phonon scattering. However, an unexpected behavior is observed for the two set of processed samples. At low temperatures, the sheet resistance of the two set of implanted and PLM samples begin to increase and are higher than the Si reference sample. This fact is not possible if we assume a parallel conduction scheme. The sheet resistance of the whole sample (TIL / Si substrate) cannot be higher than one of the conduction branches (Si substrate).

Then, an electrical decoupling between the two layers seems to take place since we are only contacting electrically the TIL. For room temperature the processed samples presents the expected sheet resistance of a parallel double sheet conduction scheme (TIL / Si substrate).

To explain these results we show in Fig. 4 a band diagram of the double sheet structure TIL / n-Si substrate at 300 K and at 100 K as it should be like according to the IB theory. In this structure we assume the IB formation in the TIL. It is expected that the Fermi level should be pinned at the IB energy in the TIL since the IB would have a high density of states. Then, the carrier concentration at the CB and VB should be determined by the Maxwell-Boltzmann statistics and their densities are going to be strongly dependent of the temperature. At 300 K, the thermal energy is enough to promote charge carriers from the IB to the CB in the TIL, while in the n-Si substrate we have the extrinsic charge carrier concentration as is expected with a shallow donor level n-Si substrate. In this situation the current flow is possible in both senses, from the TIL to the n-Si substrate and from the n-Si substrate to the TIL. That is, the bilayer is electrically coupled.

In a previous complete electrical characterization we have calculated by means of an analytical bilayer model that the energy position of the IB is at 0.38 eV from the CB [13]. This analytical bilayer model has been fitted correctly to the experimental sheet resistance measurements. We have obtained almost the same adjusting parameters (specifically, the energy location of the IB) for the simple implanted and for the double implanted samples. At 100 K, the Maxwell-Boltzmann statistic give us a negligibly electron concentration in the CB of the TIL. In this situation electrons flow from TIL to the n-Si substrate is not possible. Furthermore the IB is totally isolated. These facts imply the most important blocking characteristic to the flow of current and explain the electrical decoupling observed in the bilayer.

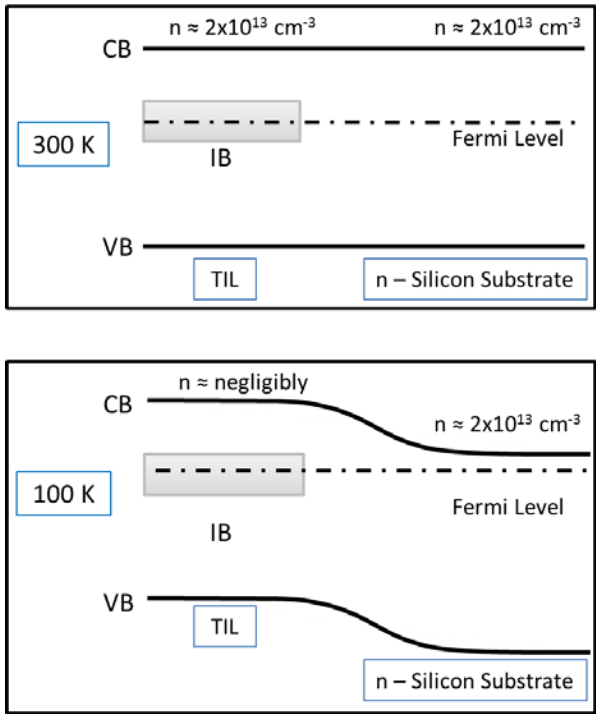

FIGURE 4. Band diagrams of the TIL/n-Si substrate structure at 300 K and 100 K.

On the other hand, as the temperature decreases the Fermi level in the n-Si substrate has to be closer to the CB and become to bend the n-Si substrate bands. This bending would suppose a potential barrier to the electron flow from the n-Si substrate to the TIL. As in the room temperature case, in the CB of the n-Si substrate we have the charge carrier concentration expected for the shallow donor level still fully activated.

The IB formation in the Ti implanted layer can explain satisfactorily the electrical decoupling observed in the processed samples.

CONCLUSIONS

In this paper we have presented the technological challenges that involve the fabrication of an IB material. We have used the combination of out of thermodynamical equilibrium techniques as the ion implantation and PLM, to obtain Ti concentrations above the limit to IB formation with a high crystal quality. Ti concentration profiles obtained from ToF-SIMS measurements show a Ti concentration about 2-4x10^{20} cm^{-3}, well above the theoretical Mott limit and six orders of magnitude higher than the solid solubility limit of Ti in Si. From the point of view of a photovoltaic device application, we have obtained an active layer of 120 nm of thickness for the sample with the double implantation, which is clearly higher than the 20 nm obtained for the sample with a single implantation. By means of sheet resistance measurements as a function of the temperature, we find an anomalous electrical decoupling for the two processed samples. This unusual behavior has been successfully explained taking into account an IB formation in the Ti supersaturated Si layer. These results points out that thicker layer of the active IB material can be obtained by the combined use of ion implantation and PLM processes.

ACKNOWLEDGMENTS

Authors would like to acknowledge the CAI de Técnicas Físicas of the Universidad Complutense de Madrid for the ion implantations and metallic evaporations and the Nanotechnology and Surface Analysis Services of the Universidad de Vigo C.A.C.T.I. for ToF-SIMS measurements. This work was partially supported by the Project NUMANCIA II (Grant No. S-2009/ENE/1477) funded by the Comunidad de Madrid. Research by E. Garcia-Hemme, was also supported by a PICATA predoctoral fellowship of the Moncloa Campus of International Excellence (UCM-UPM). J. Olea and D. Pastor thanks Prof. A. Martí and Prof. A. Luque for useful discussions and guidance and acknowledge financial support from the MICINN within the program Juan de la Cierva (JCI-2011-10402 and JCI-2011-11471), under which this research was undertaken.

REFERENCES

1. A. Luque and A. Marti, Phys. Rev. Lett. **78** (26), 5014-5017 (1997).
2. A. Marti *et al*. Thin Solid Films **511**, 638-644 (2006).
3. J. Wu, W. Shan and W. Walukiewicz, Semicond. Sci. Tech. **17** (8), 860-869 (2002).
4. E. Antolin *et al*. Appl. Phys. Lett. **94** (4), 042115 (2009).
5. A. Luque *et al.* Phys. B-Cond. Matter **382** (1-2), 320-327 (2006).
6. K. Sanchez *et al.* Phys. Rev. B **79** (16), 165203 (2009).
7. S. Hocine and D. Mathiot, Appl. Phys. Lett. **53** (14), 1269-1271 (1988).
8. C. W. White *et al.* J. Appl. Phys. **51** (1), 738-749 (1980).
9. J. Olea *et al*. J. Appl. Phys. **104** (1), 016105 (2008).
10. J. Olea *et al*. J. Appl. Phys. **109** (11), 113541 (2011).
11. J. Olea *et al*. J. Appl. Phys. **107** (10), 103524 (2010).
12. D. Pastor *et al*. Semicond. Sci. Tech. **26** (11) (2011).
13. J. Olea *et al*. J. Appl. Phys. **109** (6), 8 (2011).